

Large stable oscillations due to Hopf bifurcations in amplitude dynamics of colliding soliton sequences

Avner Peleg¹, Debananda Chakraborty²

¹ *Department of Exact Sciences, Afeka College of Engineering, Tel Aviv 69988, Israel*

² *Department of Mathematics, New Jersey City University,
Jersey City, New Jersey 07305, USA*

(Dated: March 26, 2022)

Abstract

We demonstrate that the amplitudes of optical solitons in nonlinear multisequence optical waveguide coupler systems with weak linear and cubic gain-loss exhibit large stable oscillations along ultra-long distances. The large stable oscillations are caused by supercritical Hopf bifurcations of the equilibrium states of the Lotka-Volterra (LV) models for dynamics of soliton amplitudes. The predictions of the LV models are confirmed by numerical simulations with the coupled cubic nonlinear Schrödinger (NLS) propagation models with $2 \leq N \leq 4$ pulse sequences. Thus, we provide the first demonstration of intermediate nonlinear amplitude dynamics in multisequence soliton systems, described by the cubic NLS equation. Our findings are also an important step towards realization of spatio-temporal chaos with multiple periodic sequences of colliding NLS solitons.

PACS numbers: 42.65.Tg, 42.65.Sf, 05.45.Yv

I. INTRODUCTION

The cubic nonlinear Schrödinger (NLS) equation, which describes wave propagation in the presence of second-order dispersion and cubic (Kerr) nonlinearity, is one of the most widely used nonlinear wave models in physics. It was successfully employed to describe water wave dynamics [1, 2], Bose-Einstein condensates [3, 4], and pulse propagation in nonlinear optical waveguides [5, 6]. The fundamental NLS solitons are the most ubiquitous solutions of the cubic NLS equation due to their stability. Indeed, stable dynamics of single NLS solitons and of a single periodic sequence of NLS solitons has been observed in a wide range of physical systems [1–6]. However, the situation is very different for propagation of multiple periodic soliton sequences. Such multisequence propagation setups are of particular interest in nonlinear broadband (multichannel) optical waveguide systems [5–7]. In these waveguide systems, the solitons in each periodic sequence propagate with the same frequency and group velocity, but the frequency and group velocity are different for solitons from different sequences [5–7]. As a result, intersequence soliton collisions are frequent and can lead to significant amplitude and frequency shifts and to severe transmission degradation. In fact, multichannel transmission with NLS solitons is unstable due to resonant emission of small-amplitude waves [7–9]. Considering the ubiquity of the fundamental NLS soliton and of the single soliton sequence, the fact that stable long-distance propagation of multiple sequences of fundamental solitons has not been demonstrated in any system described by the cubic NLS equation is quite troubling. In particular, one would not expect intermediate or strongly nonlinear dynamics of soliton amplitudes in these systems.

In Refs. [9–14], we developed a general method for stabilizing dynamics of soliton amplitudes in nonlinear multisequence optical waveguide systems with nonlinear dissipation. The method is based on showing that amplitude dynamics induced by nonlinear dissipation in N -sequence waveguide systems can be approximately described by N -dimensional Lotka-Volterra (LV) models. Stability analysis of the equilibrium states of the LV models can then be used for realizing stable amplitude dynamics along ultra-long distances. However, due to the inherent instability of multichannel soliton-based transmission against radiation emission, the distances along which stable amplitude dynamics was observed in numerical simulations were initially limited to a few hundred dispersion lengths [11, 12]. Significant increase in the stable propagation distances was enabled by the introduction of frequency

dependent linear gain-loss in N -waveguide couplers [8, 9]. The limiting cause for transmission instability in the latter systems was associated with radiation emission due to the effects of dissipative perturbations on single-soliton propagation [9]. Therefore, this process is a serious obstacle for observing intermediate and strongly nonlinear amplitude dynamics in multichannel transmission with NLS solitons. Indeed, in all previous studies of multichannel soliton-based transmission, the dissipation-induced amplitude dynamics was only weakly nonlinear [9–14]. Furthermore, intermediate or strongly nonlinear amplitude dynamics has not yet been demonstrated in any multisequence soliton system, described by the cubic NLS equation.

A common mechanism for inducing intermediate nonlinear dynamics is by means of supercritical Hopf bifurcations [15–18]. In this case, as the value of a physical parameter is changed beyond some threshold value, a stable equilibrium state of the dynamical model becomes unstable, and a stable limit cycle about the unstable equilibrium state appears [15, 16]. As a result, for parameter values larger than the threshold value, the system exhibits stable oscillations with relatively large amplitudes, i.e., intermediate nonlinear amplitude dynamics. Supercritical Hopf bifurcations occur in many physical systems, including electric circuits [16], chemical reactions [17–19], and population dynamics [18, 20–25]. Here, we are interested in LV models, which describe dynamics of population sizes [18, 26, 27] as well as the time evolution of chemical concentrations in certain chemical reactions [17–19, 28, 29]. The occurrence of supercritical Hopf bifurcations in LV models is of special interest, since in some cases, as the value of the bifurcation parameter is further changed, the limit cycle undergoes a period doubling cascade, and finally, chaotic dynamics is observed [19, 21–24].

In the current paper, we provide the first demonstration of intermediate nonlinear dynamics of soliton amplitudes in multisequence soliton systems, described by the cubic NLS equation. For this purpose, we study propagation of multiple periodic soliton sequences in nonlinear optical waveguide coupler systems with weak linear gain-loss, weak broadband cubic gain-loss, and narrowband Kerr nonlinearity. The values of the gain-loss coefficients are chosen such that the equilibrium states of the LV models for amplitude dynamics undergo supercritical Hopf bifurcations. This enables observation of large stable oscillations of soliton amplitudes along ultra-long distances. The narrowband nature of the Kerr nonlinearity and the broadband nature of the cubic gain-loss lead to enhanced pulse pattern stability

compared with the waveguides considered in Refs. [9–14]. Since two of the LV models that we study exhibit chaotic dynamics, our findings are an important step towards realization of spatio-temporal chaos with multiple sequences of colliding NLS solitons.

The rest of the paper is organized as follows. In Section II, we present the coupled-NLS models for pulse propagation and the LV models for dynamics of soliton amplitudes. In Section III, we present four examples for multisequence waveguide coupler systems, in which the soliton amplitudes exhibit large stable oscillations along ultra-long distances. For each of the four systems we present the predictions of the LV models, the results of numerical simulations with the coupled-NLS models, and a comparison. Our conclusions are presented in Section IV.

II. COUPLED-NLS AND LV MODELS

A. Coupled-NLS propagation models

We consider propagation of N sequences of optical pulses in an optical waveguide coupler, consisting of N close waveguides, where each sequence propagates through its own waveguide. We assume a multisequence setup, where the pulses in each sequence propagate with the same group velocity, but where the group velocity is different for pulses from different sequences [5–7]. Additionally, we assume that the sequences propagate in the presence of second-order dispersion, Kerr nonlinearity, and weak linear and cubic gain-loss. Thus, the propagation is described by the following system of N coupled cubic NLS equations [5, 8, 11, 30]:

$$\begin{aligned}
 i\partial_z\psi_j + \partial_t^2\psi_j + 2|\psi_j|^2\psi_j &= i\mathcal{F}^{-1}(G_j(\omega, z)\hat{\psi}_j)/2 \\
 -2i\sum_{k=1}^N(1 - \delta_{jk})\epsilon_{3jk}|\psi_k|^2\psi_j, & \quad (1)
 \end{aligned}$$

where ψ_j is the envelope of the electric field of the j th sequence, $1 \leq j \leq N$, z is propagation distance, t is time, and ω is frequency [31]. In Eq. (1), $G_j(\omega, z)$ is the linear gain-loss experienced by j th sequence pulses, $\hat{\psi}_j$ is the Fourier transform of ψ_j with respect to time, \mathcal{F}^{-1} is the inverse Fourier transform, and δ_{jk} is the Kronecker delta function. The coefficients ϵ_{3jk} , which describe the strength of cubic gain-loss interaction between j th and k th sequence pulses, satisfy $|\epsilon_{3jk}| \ll 1$. The second and third terms on the left hand side of Eq. (1) describe

second-order dispersion effects and intrasequence interaction due to Kerr nonlinearity. The first term on the right hand side of Eq. (1) describes the effects of frequency dependent linear gain-loss, while the second term corresponds to intersequence interaction due to cubic gain-loss. We assume that Kerr nonlinearity is narrowband, i.e., that it is negligible for frequency differences that are much larger than the spectral width of the pulses. In addition, we assume that cubic gain-loss is broadband, i.e., that it is non-negligible only for frequency differences that are much larger than the spectral width of the pulses. As a result, we can neglect interchannel interaction due to Kerr nonlinearity and intrachannel interaction due to cubic gain-loss. These properties, which are new compared with the waveguides studied in all previous works on multichannel soliton-based transmission [8, 9, 11–14], lead to significant enhancement of pulse pattern stability and enable the observation of large stable oscillations of pulse amplitudes along ultra-long distances in simulations with Eq. (1).

The k th pulse in the j th sequence is a fundamental soliton of the unperturbed NLS equation $i\partial_z\psi_{jk} + \partial_t^2\psi_{jk} + 2|\psi_{jk}|^2\psi_{jk} = 0$. The envelope of this soliton is $\psi_{sjk}(t, z) = \eta_j \exp(i\chi_{jk})\text{sech}(x_{jk})$, where $x_{jk} = \eta_j(t - y_{jk} - 2\beta_j z)$, $\chi_{jk} = \alpha_j + \beta_j(t - y_{jk}) + (\eta_j^2 - \beta_j^2)z$, and η_j , β_j , y_{jk} , and α_j are the soliton amplitude, frequency, position, and phase. In a periodic sequence with index j , the positions of the k th and $(k+1)$ th pulses in the sequence are related by $y_{jk} = y_{j,k-1} + T$, where T is the intrasequence separation between adjacent pulses.

The form of the linear gain-loss $G_j(\omega, z)$ is chosen such that large stable oscillations of soliton amplitudes are enabled, while pulse pattern destabilization due to radiation emission is suppressed. In particular, we choose a form similar to the one that was used in Refs. [8, 9, 32]:

$$G_j(\omega, z) = \begin{cases} \epsilon_1 g_j(z) & \text{if } \beta_j(0) - W/2 < \omega \leq \beta_j(0) + W/2, \\ -g_L & \text{elsewhere,} \end{cases} \quad (2)$$

where ϵ_1 is the linear gain coefficient, $0 < \epsilon_1 \ll 1$, $\beta_j(0)$ is the initial frequency of j th sequence solitons, and g_L is an $O(1)$ positive constant. The spectral width W in Eq. (2) satisfies $1 < W \leq \Delta\beta$, where the frequency spacing $\Delta\beta$ is defined by: $\Delta\beta = \beta_{j+1}(0) - \beta_j(0)$ for $1 \leq j \leq N - 1$. The function $g_j(z)$ is: $g_j(z) = g_{1j} + g_{2j}\eta_j(z) + g_{3j}\eta_j^2(z)$, where $\eta_j(z)$ is the amplitude of j th sequence solitons. The values of the constants g_{1j} , g_{2j} , and g_{3j} are chosen such that the soliton amplitudes exhibit large stable oscillations due to Hopf

bifurcations of the equilibrium states of the LV models for amplitude dynamics. The strong linear loss g_L leads to efficient suppression of instability due to emission of radiation with frequencies outside the interval $(\beta_j(0) - W/2, \beta_j(0) + W/2]$. Simulations with Eq. (1) show that efficient mitigation of radiative instability is achieved for g_L and W values around 0.5 and 10, respectively. The flat gain in the interval $(\beta_j(0) - W/2, \beta_j(0) + W/2]$ can be realized by flat-gain amplifiers [33], and the strong loss outside of this interval can be achieved by filters [33] or by waveguide impurities [5].

B. LV models for dynamics of soliton amplitudes

In Refs. [9–14], we showed that amplitude dynamics of N periodic sequences of colliding solitons in nonlinear optical waveguides with weak dissipation can be described by N -dimensional LV models. The derivation of the LV models was based on the following assumptions. (1) The intrasequence separation T satisfies: $T \gg 1$. In addition, the amplitudes are equal for all solitons from the same sequence, but are not necessarily equal for solitons from different sequences. (2) The sequences are either (a) subject to periodic temporal boundary conditions or (b) infinitely long. Setup (a) corresponds to waveguide-loop experiments and setup (b) approximates long-haul transmission. (3) As $T \gg 1$, intrasequence interaction is exponentially weak and is neglected. (4) High-order radiation emission effects are also neglected.

Under these assumptions, the soliton sequences remain periodic and therefore the amplitudes of all pulses in a given sequence follow the same dynamics. Taking into account collision-induced amplitude shifts due to cubic gain-loss and single-pulse amplitude changes due to linear gain-loss, we obtain the following equation for amplitude dynamics of j th sequence solitons [11]:

$$\frac{d\eta_j}{dz} = \eta_j \left[\epsilon_1 g_j(z) - \frac{8}{T} \sum_{k=1}^N (1 - \delta_{jk}) \epsilon_{3jk} \eta_k \right]. \quad (3)$$

Equation (3) has the form of a LV model for N species [26, 27]. The choice of physical parameter values in Eq. (3) is guided by the following requirements. (a) The LV model (3) has an equilibrium state with equal or near-equal amplitudes, whose values are close to 1, when the value of the bifurcation parameter μ is close to its Hopf bifurcation value μ_H [34]. (b) The equilibrium state with near-equal amplitudes undergoes a supercritical Hopf

bifurcation at $\mu = \mu_H$. As a result, the equilibrium state changes from a stable focus to an unstable state and a stable limit cycle around the unstable state appears. The emergence of the stable limit cycle is the key factor in enabling large stable amplitude oscillations. Requirement (a) is added so that the perturbation procedure leading to Eq. (3) is valid when μ is close to μ_H . Requirements (a) and (b) are new features of the LV model and the corresponding waveguide systems and were not considered in Refs. [9–14].

III. SPECIFIC MULTISEQUENCE TRANSMISSION SETUPS LEADING TO INTERMEDIATE NONLINEAR AMPLITUDE DYNAMICS

A. Introduction

We consider four multisequence waveguide coupler systems with weak linear and cubic gain-loss as prototypical examples for waveguide systems, where dynamics of soliton amplitudes with large stable oscillations that is induced by a supercritical Hopf bifurcation can be observed. For each waveguide coupler system, we present the predictions of the LV model (3), the results of numerical simulations with the coupled-NLS model (1), and a comparison.

Equation (1) is numerically solved using the split-step method with periodic boundary conditions [5, 35]. Due to the periodic boundary conditions, the simulations describe propagation in a closed waveguide loop. The initial condition consists of N periodic sequences of $2K + 1$ solitons with amplitudes $\eta_j(0)$, frequencies $\beta_j(0)$, and zero phases:

$$\psi_j(t, 0) = \sum_{k=-K}^K \frac{\eta_j(0) \exp[i\beta_j(0)(t - kT)]}{\cosh[\eta_j(0)(t - kT)]}, \quad (4)$$

where $1 \leq j \leq N$, and $2 \leq N \leq 4$. We use $W = 10$ and $g_L = 0.5$ for the parameters of the linear gain-loss function $G_j(\omega, z)$. For concreteness, we present here the results of simulations with $T = 20$, $\Delta\beta = 40$, $K = 1$, and a final distance $z_f = 5000$. We emphasize, however, that similar results are obtained with other physical parameter values.

B. Two-sequence transmission

The two-dimensional (2D) LV model for two-sequence transmission is a variant of the predator-prey model analyzed by Odell in Ref. [20] in the context of population dynamics.

The model is given by Eq. (3) with $N=2$, $g_{11}=-\mu$, $g_{21}=g_{31}=0$, $g_{12}=-1$, $g_{22}=4$, $g_{32}=-2$, $\epsilon_{312}=-\epsilon_1 T/8$, $\epsilon_{321}=\epsilon_1 T/8$, where μ is a bifurcation parameter. Therefore, the LV model is:

$$\begin{aligned}\frac{d\eta_1}{dz} &= \epsilon_1 \eta_1 (-\mu + \eta_2), \\ \frac{d\eta_2}{dz} &= \epsilon_1 \eta_2 (-1 + 4\eta_2 - 2\eta_2^2 - \eta_1).\end{aligned}\tag{5}$$

Note that in this transmission system, the $j = 1$ sequence propagates in the presence of linear loss with coefficient $g_1 = -\mu$ and cubic gain intersequence interaction, while the $j = 2$ sequence propagates in the presence of linear gain-loss with coefficient $g_2(z) = -1 + 4\eta_j - 2\eta_j^2$ and cubic loss intersequence interaction. The equilibrium state with near-equal amplitudes is $(\eta_1^{(eq)}, \eta_2^{(eq)}) = (-1 + 4\mu - 2\mu^2, \mu)$. This state undergoes a supercritical Hopf bifurcation as μ changes through 1. For $\mu < 1$, the equilibrium state is an unstable focus, which is surrounded by a stable limit cycle, while for $\mu > 1$, it is a stable focus and the limit cycle does not exist [20]. Thus, we expect large stable amplitude oscillations for $\mu < 1$, and stable oscillations that decay to $\eta_j^{(eq)}$ for $\mu > 1$.

To test these predictions, we numerically solve Eq. (1) with $\epsilon_1 = 0.05$ for different μ values close to 1. As an example, we present here the results of the simulations with initial soliton amplitudes $\eta_1(0) = 0.95$ and $\eta_2(0) = 1.05$. Figures 1(a) and 1(b) show the z dependence of η_j obtained by the simulations for $\mu = 0.98$ and $\mu = 1.05$, respectively. The predictions of the LV model (5) are also shown. It is seen that for $\mu = 0.98$, the amplitudes exhibit large stable oscillations that approach limit cycle behavior, in very good agreement with the LV model's predictions. Additionally, for $\mu = 1.05$, the amplitudes exhibit decaying oscillations and approach their equilibrium values $\eta_j^{(eq)}$ in accordance with the LV model. Furthermore, as seen in Fig. 2, in both cases the solitons retain their shape throughout the propagation. Similar results are obtained for other values of μ and the $\eta_j(0)$.

C. Three-sequence transmission

1. A transmission setup based on the 1980 Arneodo LV model

We first consider a three-dimensional (3D) LV model for amplitude dynamics in three-sequence waveguide coupler transmission, which was studied by Arneodo et al. in Ref. [21]. The model was introduced and investigated in the context of population dynamics as an

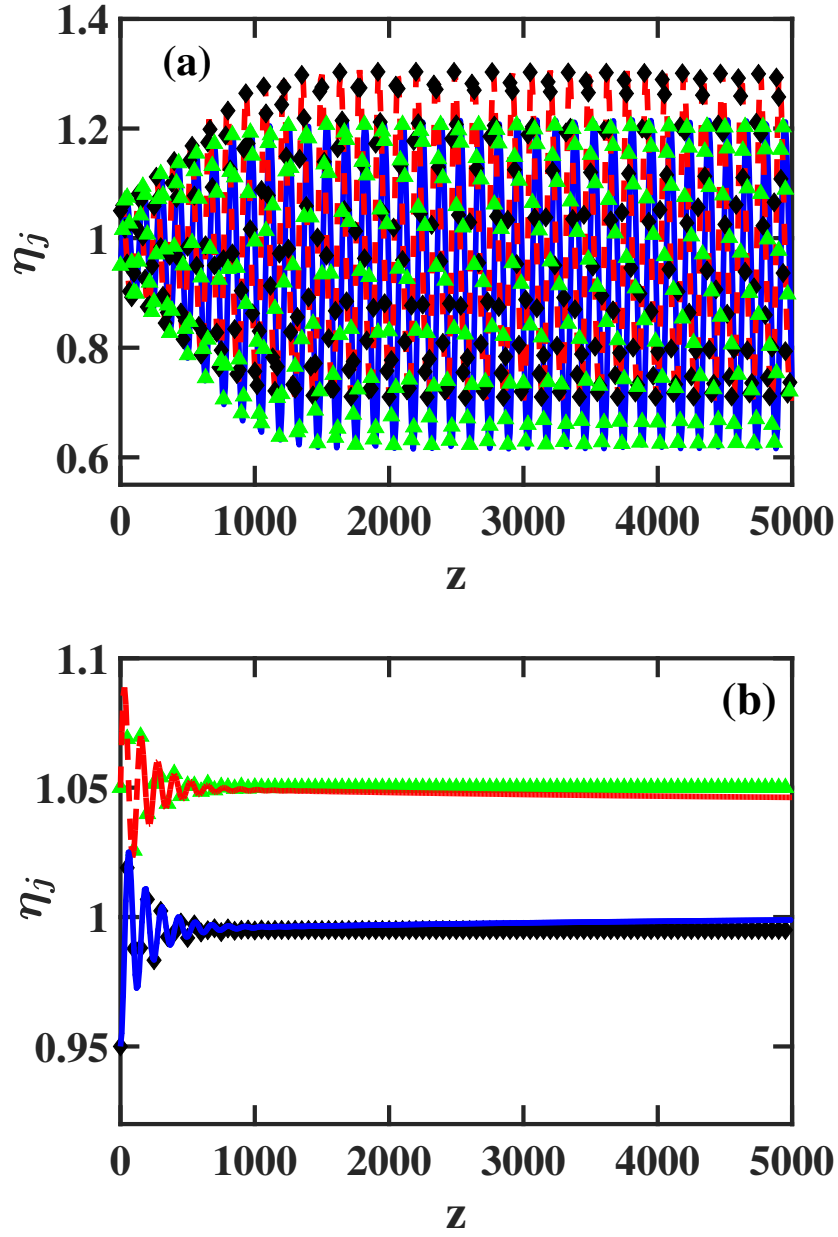


FIG. 1: (Color online) The z -dependence of soliton amplitudes η_j in the two-sequence waveguide coupler system of subsection III B for $\mu = 0.98$ (a) and $\mu = 1.05$ (b). The linear gain-loss coefficient is $\epsilon_1 = 0.05$ and the initial amplitudes are $\eta_1(0) = 0.95$ and $\eta_2(0) = 1.05$. The solid blue and dashed red curves represent $\eta_j(z)$ with $j = 1, 2$, obtained by numerical simulations with Eq. (1). The black diamonds and green triangles represent $\eta_j(z)$ with $j = 1, 2$, obtained by the LV model (5).

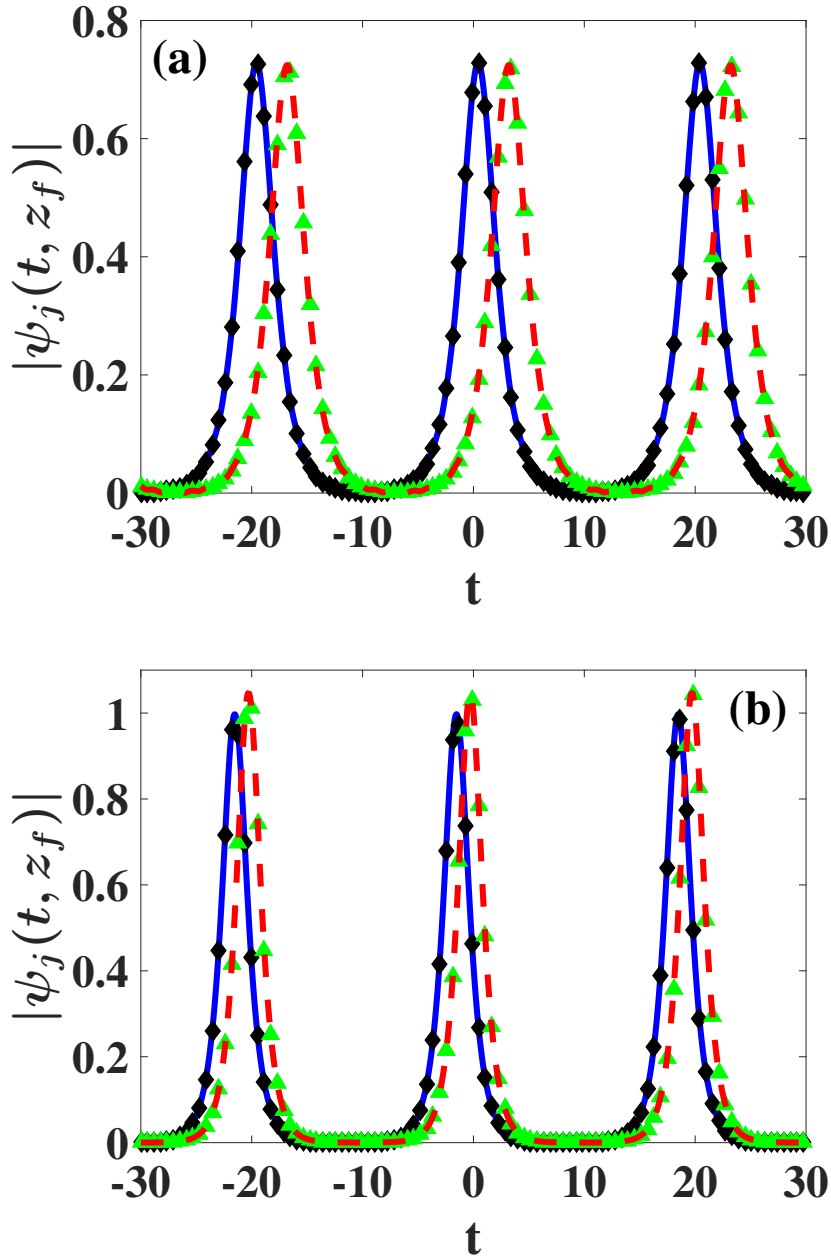


FIG. 2: (Color online) The pulse patterns at the final propagation distance $|\psi_j(t, z_f)|$, where $z_f = 5000$, for the two-sequence transmission system of subsection III B with $\mu = 0.98$ (a) and $\mu = 1.05$ (b). The parameter values are the same as in Fig. 1. The solid blue and dashed red curves correspond to $|\psi_j(t, z_f)|$ with $j = 1, 2$, obtained by numerical simulations with Eq. (1). The black diamonds and green triangles correspond to the theoretical prediction, obtained by summation over fundamental NLS solitons.

example for a low-dimensional LV system exhibiting chaos. The model is given by Eq. (3) with $N = 3$, $g_{11} = 1.1$, $g_{21} = -0.5$, $g_{12} = -0.5$, $g_{22} = 0.1$, $g_{13} = 0.2 + \mu$, $g_{23} = -0.1$, $g_{31} = g_{32} = g_{33} = 0$, $\epsilon_{312} = 0.5\epsilon_1 T/8$, $\epsilon_{313} = 0.1\epsilon_1 T/8$, $\epsilon_{321} = -0.5\epsilon_1 T/8$, $\epsilon_{323} = 0.1\epsilon_1 T/8$, $\epsilon_{331} = \mu\epsilon_1 T/8$, $\epsilon_{332} = 0.1\epsilon_1 T/8$. Thus, this LV model is:

$$\begin{aligned}\frac{d\eta_1}{dz} &= \epsilon_1 \eta_1 (1.1 - 0.5\eta_1 - 0.5\eta_2 - 0.1\eta_3), \\ \frac{d\eta_2}{dz} &= \epsilon_1 \eta_2 (-0.5 + 0.5\eta_1 + 0.1\eta_2 - 0.1\eta_3), \\ \frac{d\eta_3}{dz} &= \epsilon_1 \eta_3 (0.2 + \mu - \mu\eta_1 - 0.1\eta_2 - 0.1\eta_3).\end{aligned}\quad (6)$$

Note that in this waveguide coupler system, sequences $j = 1$ and $j = 3$ propagate in the presence of cubic loss intersequence interaction, while the $j = 2$ sequence propagates in the presence of cubic gain intersequence interaction with sequence $j = 1$ and cubic loss intersequence interaction with sequence $j = 3$. The relevant equilibrium state of the LV model is $(1, 1, 1)$, independent of the value of μ [21]. This equilibrium state undergoes a supercritical Hopf bifurcation as μ increases through $\mu_H \simeq 0.954$ [21]. As a result, for $\mu < \mu_H$, the equilibrium state is a stable focus, while for $\mu > \mu_H$, $(1, 1, 1)$ becomes unstable and a stable limit cycle about $(1, 1, 1)$ appears. As μ increases beyond $\mu_P \simeq 1.265$, the limit cycle undergoes a period doubling cascade, and finally, chaotic dynamics is observed [21]. Thus, we expect the amplitudes to exhibit stable decaying oscillations and approach the equilibrium value 1 for $\mu < \mu_H$, and to exhibit large stable oscillations with a single period for $\mu_H < \mu < \mu_P$.

To validate the predictions of the LV model, we numerically solve Eq. (1) with $\epsilon_1 = 0.1$ for different μ values. As an example, we present here the results of the simulations with initial amplitudes $\eta_1(0) = 0.95$, $\eta_2(0) = 1.05$, and $\eta_3(0) = 1.2$. Figures 3(a) and 3(b) show the z dependence of η_j obtained by the simulations for $\mu = 0.85$ and $\mu = 0.98$, respectively, together with the predictions of the LV model (6). The agreement between the numerical simulations and the predictions of the LV model is very good for both values of μ . In particular, for $\mu = 0.85$, the amplitudes exhibit decaying oscillations and approach their equilibrium value of 1, while for $\mu = 0.98$, the amplitudes exhibit large stable oscillations that tend to limit cycle behavior. Furthermore, as seen in Fig. 4, in both cases the soliton patterns remain intact throughout the propagation. Similar results are obtained for other values of μ and the $\eta_j(0)$.

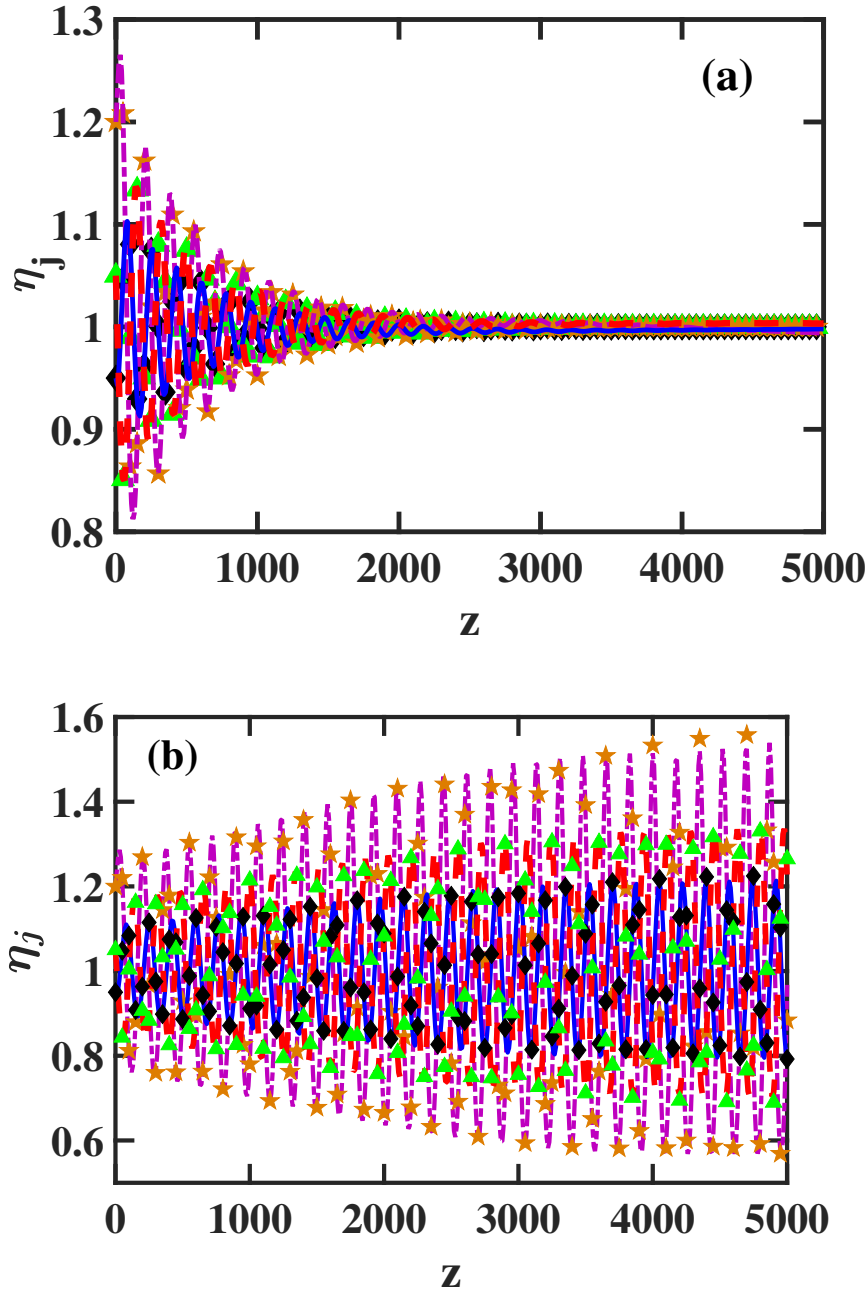


FIG. 3: (Color online) The z -dependence of soliton amplitudes η_j in the three-sequence waveguide coupler system of subsection III C 1 for $\mu = 0.85$ (a) and $\mu = 0.98$ (b). The linear gain-loss coefficient is $\epsilon_1 = 0.1$ and the initial amplitudes are $\eta_1(0) = 0.95$, $\eta_2(0) = 1.05$, and $\eta_3(0) = 1.2$. The solid blue, dashed red, and dash-dotted purple curves represent $\eta_j(z)$ with $j = 1, 2, 3$, obtained by numerical simulations with Eq. (1). The black diamonds, green triangles, and orange stars represent $\eta_j(z)$ with $j = 1, 2, 3$, obtained by the LV model (6).

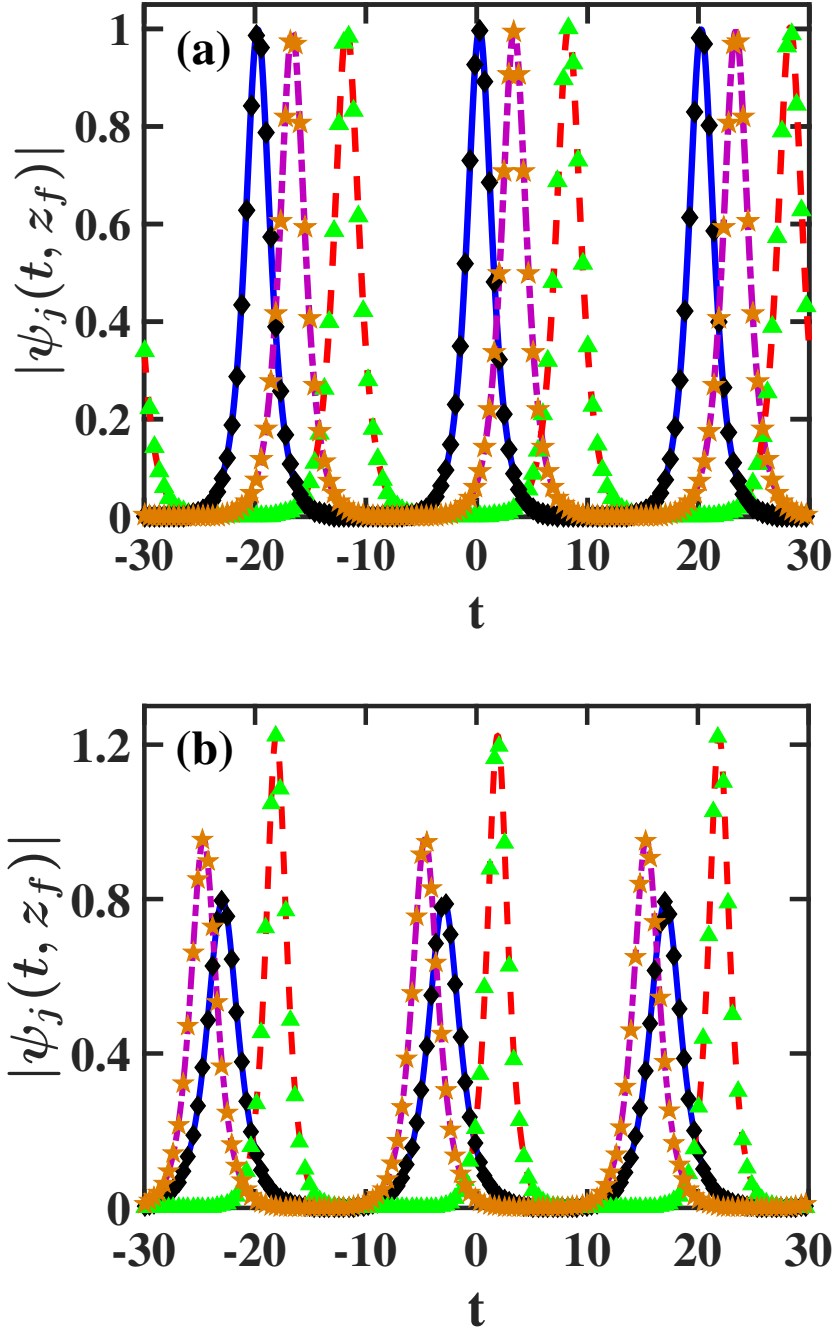


FIG. 4: (Color online) The pulse patterns at the final propagation distance $|\psi_j(t, z_f)|$, where $z_f = 5000$, for the three-sequence transmission system of subsection III C 1 with $\mu = 0.85$ (a) and $\mu = 0.98$ (b). The parameter values are the same as in Fig. 3. The solid blue, dashed red, and dash-dotted purple curves correspond to $|\psi_j(t, z_f)|$ with $j = 1, 2, 3$, obtained by numerical simulations with Eq. (1). The black diamonds, green triangles, and orange stars correspond to the theoretical prediction, obtained by summation over fundamental NLS solitons.

2. A simpler three-sequence transmission setup

We now consider a second example for a 3D LV model for amplitude dynamics in three-sequence waveguide coupler transmission, for which the soliton amplitudes exhibit large stable oscillations due to a supercritical Hopf bifurcation. This 3D LV model does not exhibit chaotic dynamics, but it has the advantage of having a simpler form compared with the 3D model of Eq. (6). The model is given by Eq. (3) with $N = 3$, $g_{11} = -2\mu$, $g_{21} = 0$, $g_{12} = 0$, $g_{22} = -1$, $g_{13} = 2$, $g_{23} = -1$, $g_{31} = g_{32} = g_{33} = 0$, $\epsilon_{312} = 0$, $\epsilon_{313} = -\epsilon_1 T/4$, $\epsilon_{321} = -\epsilon_1 T/8$, $\epsilon_{323} = 0$, $\epsilon_{331} = 0$, $\epsilon_{332} = \epsilon_1 T/8$. Therefore, the LV model is:

$$\begin{aligned}\frac{d\eta_1}{dz} &= 2\epsilon_1\eta_1(-\mu + \eta_3), \\ \frac{d\eta_2}{dz} &= \epsilon_1\eta_2(\eta_1 - \eta_2), \\ \frac{d\eta_3}{dz} &= \epsilon_1\eta_3(2 - \eta_2 - \eta_3).\end{aligned}\tag{7}$$

In this waveguide coupler system, sequences $j = 1$ and $j = 2$ propagate in the presence of cubic gain intersequence interaction, while the $j = 3$ sequence propagates in the presence of cubic loss intersequence interaction. The relevant equilibrium state is $(\eta_1^{(eq)}, \eta_2^{(eq)}, \eta_3^{(eq)}) = (2 - \mu, 2 - \mu, \mu)$. Stability analysis shows that this equilibrium state undergoes a supercritical Hopf bifurcation as μ changes through 1. For $0 < \mu < 1$, the equilibrium state is an unstable focus, which is surrounded by a stable limit cycle. Additionally, for $1 < \mu < 2$, it is a stable focus and the limit cycle does not exist. Therefore, we expect large stable amplitude oscillations for $0 < \mu < 1$, and stable oscillations that decay to $\eta_j^{(eq)}$ for $1 < \mu < 2$.

To check the predictions of the LV model, we numerically solve Eq. (1) with $\epsilon_1 = 0.05$ for different μ values. As an example, we present here the results of the simulations with initial soliton amplitudes $\eta_1(0) = 0.9$, $\eta_2(0) = 1.2$, and $\eta_3(0) = 0.95$. Figures 5(a) and 5(b) show the z dependence of η_j obtained by the simulations for $\mu = 0.98$ and $\mu = 1.05$, respectively, along with the predictions of the LV model (7). The agreement between the numerical simulations and the predictions of the LV model is very good for both values of μ . In particular, for $\mu = 0.98$, the amplitudes exhibit large stable oscillations that tend to limit cycle behavior, while for $\mu = 1.05$, the amplitudes exhibit decaying oscillations and approach their equilibrium values $\eta_j^{(eq)}$. Furthermore, as seen in Fig. 6, for both values of μ , the solitons retain their shape throughout the propagation. Similar results are obtained for other values of μ and the $\eta_j(0)$.

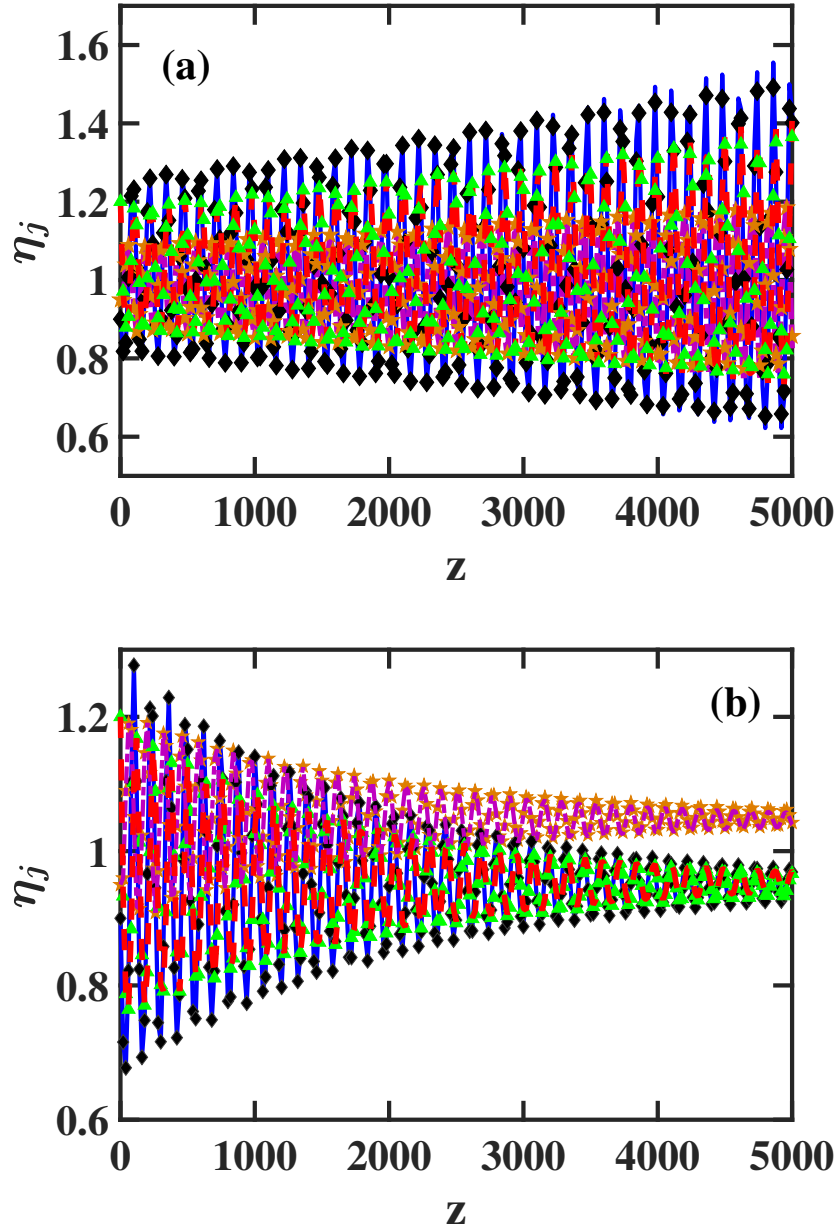


FIG. 5: (Color online) The z -dependence of soliton amplitudes η_j in the three-sequence waveguide coupler system of subsection III C 2 for $\mu = 0.98$ (a) and $\mu = 1.05$ (b). The linear gain-loss coefficient is $\epsilon_1 = 0.05$ and the initial amplitudes are $\eta_1(0) = 0.9$, $\eta_2(0) = 1.2$, and $\eta_3(0) = 0.95$. The solid blue, dashed red, and dash-dotted purple curves represent $\eta_j(z)$ with $j = 1, 2, 3$, obtained by numerical simulations with Eq. (1). The black diamonds, green triangles, and orange stars represent $\eta_j(z)$ with $j = 1, 2, 3$, obtained by the LV model (7).

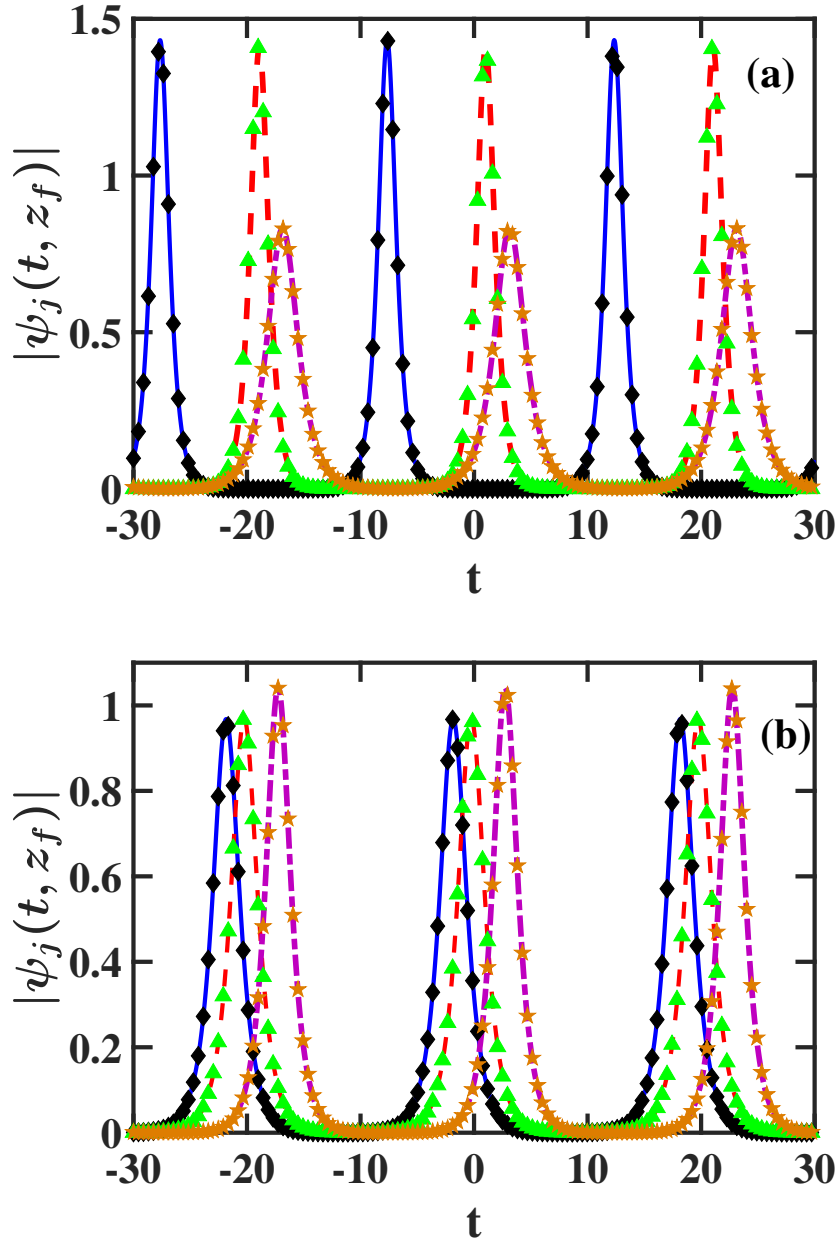


FIG. 6: (Color online) The pulse patterns at the final propagation distance $|\psi_j(t, z_f)|$, where $z_f = 5000$, for the three-sequence transmission system of subsection III C 2 with $\mu = 0.98$ (a) and $\mu = 1.05$ (b). The parameter values are the same as in Fig. 5. The solid blue, dashed red, and dash-dotted purple curves correspond to $|\psi_j(t, z_f)|$ with $j = 1, 2, 3$, obtained by numerical simulations with Eq. (1). The black diamonds, green triangles, and orange stars correspond to the theoretical prediction, obtained by summation over fundamental NLS solitons.

D. Four-sequence transmission

The four-dimensional (4D) LV model for four-sequence waveguide coupler transmission was studied in Ref. [22] in the context of population dynamics by Arneodo et al. This LV model is given by Eq. (3) with $N = 4$, $g_{1j} = 3.3$ for $j = 1, 2, 3, 4$, $g_{21} = -1$, $g_{22} = -0.4$, $g_{23} = -0.6$, $g_{24} = -1.8$, $g_{3j} = 0$ for $j = 1, 2, 3, 4$, $\epsilon_{312} = \epsilon_1 T/8$, $\epsilon_{313} = 0.6\epsilon_1 T/8$, $\epsilon_{314} = 0.7\epsilon_1 T/8$, $\epsilon_{321} = 0$, $\epsilon_{323} = 0.6\epsilon_1 T/8$, $\epsilon_{324} = 2.3\epsilon_1 T/8$, $\epsilon_{331} = (\mu + 0.5)\epsilon_1 T/8$, $\epsilon_{332} = 0.6\epsilon_1 T/8$, $\epsilon_{334} = (1.6 - \mu)\epsilon_1 T/8$, and $\epsilon_{34j} = 0.5\epsilon_1 T/8$ for $j = 1, 2, 3, 4$. Therefore, this LV model is:

$$\begin{aligned}\frac{d\eta_1}{dz} &= \epsilon_1 \eta_1 (3.3 - \eta_1 - \eta_2 - 0.6\eta_3 - 0.7\eta_4), \\ \frac{d\eta_2}{dz} &= \epsilon_1 \eta_2 (3.3 - 0.4\eta_2 - 0.6\eta_3 - 2.3\eta_4), \\ \frac{d\eta_3}{dz} &= \epsilon_1 \eta_3 [3.3 - (\mu + 0.5)\eta_1 - 0.6\eta_2 - 0.6\eta_3 - (1.6 - \mu)\eta_4], \\ \frac{d\eta_4}{dz} &= \epsilon_1 \eta_4 (3.3 - 0.5\eta_1 - 0.5\eta_2 - 0.5\eta_3 - 1.8\eta_4).\end{aligned}\tag{8}$$

Note that in this transmission system, all soliton sequences propagate in the presence of cubic loss intersequence interaction. This is very different from the two-sequence and three-sequence systems considered in the preceding subsections, where at least one of the soliton sequences propagated in the presence of cubic gain interaction. The 4D LV model (8) is in fact equivalent to the 3D LV (6) (see Ref. [36]). Therefore, the relevant equilibrium state for amplitude dynamics is $(1, 1, 1, 1)$. This equilibrium state undergoes a supercritical Hopf bifurcation at $\mu_H \simeq 0.954$ [22], and as a result, the state $(1, 1, 1, 1)$ turns from a stable focus to an unstable state and a stable limit cycle about $(1, 1, 1, 1)$ appears. As μ is increased beyond $\mu_P \simeq 1.265$, the limit cycle undergoes a period doubling cascade, and finally, chaotic dynamics is observed [22]. Thus, we expect the soliton amplitudes to exhibit stable decaying oscillations and approach 1 for $\mu < \mu_H$, and to exhibit large stable oscillations with a single period for $\mu_H < \mu < \mu_P$.

To check the predictions of the 4D LV model, we numerically solve Eq. (1) with $\epsilon_1 = 0.05$ for different μ values. As an example, we present here the results of the simulations with initial pulse amplitudes $\eta_1(0) = 0.9$, $\eta_2(0) = 1.2$, $\eta_3(0) = 0.95$, and $\eta_4(0) = 1.15$. Figures 7(a) and 7(b) show the z dependence of η_j obtained by the simulations for $\mu = 0.85$ and $\mu = 0.98$, respectively. The predictions of the LV model (8) are also shown. We find that for $\mu = 0.85$, the amplitudes exhibit decaying oscillations and approach their equilibrium

value of 1, in accordance with the LV model. Furthermore, for $\mu = 0.98$, the amplitudes exhibit large stable oscillations that tend to limit cycle behavior in very good agreement with the LV model's predictions. In addition, as seen in Fig. 8, for both values of μ the soliton patterns remain intact throughout the propagation. Similar results are obtained for other values of μ and the $\eta_j(0)$.

IV. CONCLUSIONS

We demonstrated that the amplitudes of optical solitons in multisequence nonlinear waveguide coupler systems with weak linear and cubic gain-loss exhibit large stable oscillations along ultra-long distances. The stable oscillations were caused by supercritical Hopf bifurcations of the equilibrium states of the LV models for dynamics of soliton amplitudes. The predictions of the LV models were confirmed by numerical simulations with the coupled cubic NLS propagation models with $2 \leq N \leq 4$ soliton sequences. Our results provide the first demonstration of intermediate nonlinear amplitude dynamics in multisequence soliton systems, described by the cubic NLS equation. Moreover, since two of the LV models that we studied exhibit chaotic dynamics, our results are also an important step towards the first realization of spatio-temporal chaos with multiple periodic sequences of colliding NLS solitons.

-
- [1] S. Novikov, S.V. Manakov, L.P. Pitaevskii, and V.E. Zakharov, *Theory of Solitons: The Inverse Scattering Method* (Plenum, New York, 1984).
 - [2] A.C. Newell, *Solitons in Mathematics and Physics* (SIAM, Philadelphia, 1985).
 - [3] F. Dalfovo, S. Giorgini, L.P. Pitaevskii, and S. Stringari, *Rev. Mod. Phys.* **71**, 463 (1999).
 - [4] R. Carretero-González, D.J. Frantzeskakis, and P.G. Kevrekidis, *Nonlinearity* **21**, R139 (2008).
 - [5] G.P. Agrawal, *Nonlinear Fiber Optics* (Academic, San Diego, CA, 2001).
 - [6] L.F. Mollenauer and J.P. Gordon, *Solitons in Optical Fibers: Fundamentals and Applications* (Academic, San Diego, CA, 2006).
 - [7] L.F. Mollenauer and P.V. Mamyshev, *IEEE J. Quantum Electron.* **34**, 2089 (1998).
 - [8] D. Chakraborty, A. Peleg, and Q.M. Nguyen, *Opt. Commun.* **371**, 252 (2016).

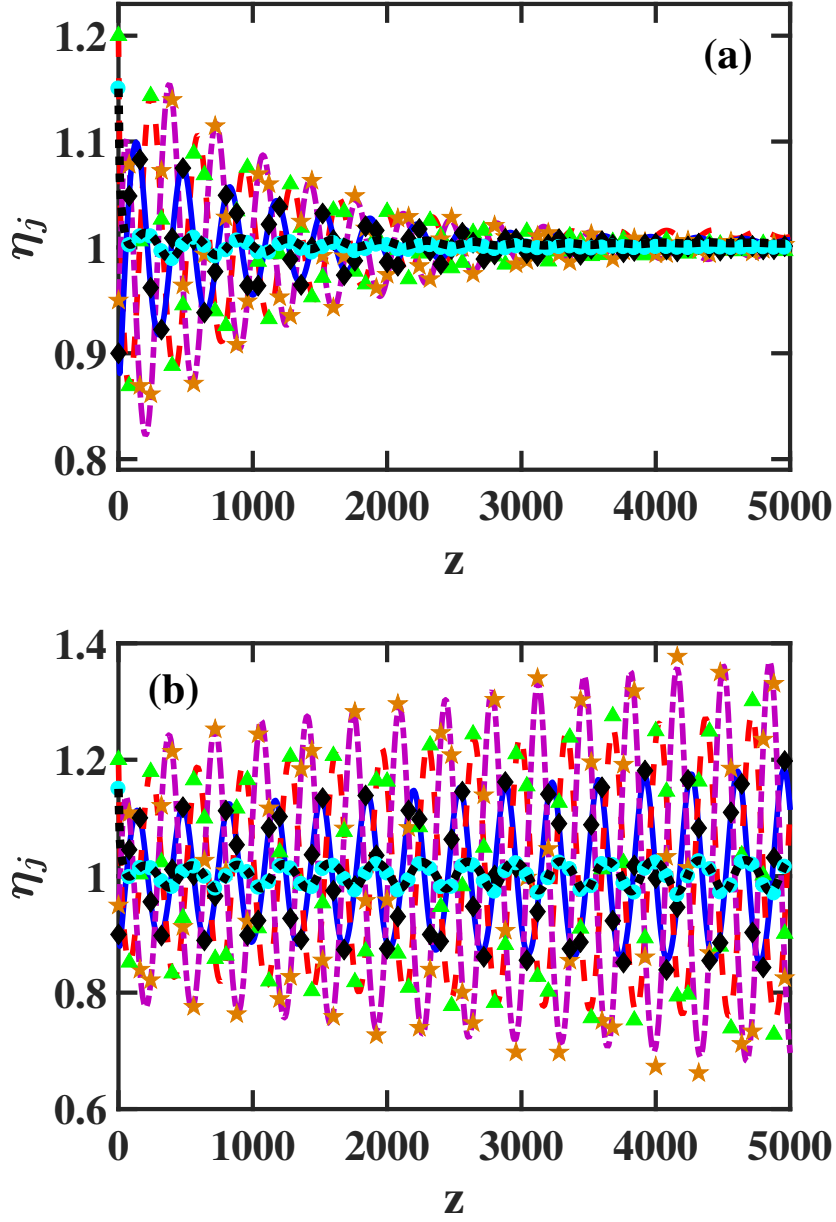


FIG. 7: (Color online) Soliton amplitudes η_j vs z in the four-sequence waveguide coupler system of subsection IIID for $\mu = 0.85$ (a) and $\mu = 0.98$ (b). The linear gain-loss coefficient is $\epsilon_1 = 0.05$ and the initial amplitudes are $\eta_1(0) = 0.9$, $\eta_2(0) = 1.2$, $\eta_3(0) = 0.95$, and $\eta_4(0) = 1.15$. The solid blue, dashed red, dash-dotted purple, and dotted black curves represent $\eta_j(z)$ with $j = 1, 2, 3, 4$, obtained by numerical simulations with Eq. (1). The black diamonds, green triangles, orange stars, and cyan circles represent $\eta_j(z)$ with $j = 1, 2, 3, 4$, obtained by the LV model (8).

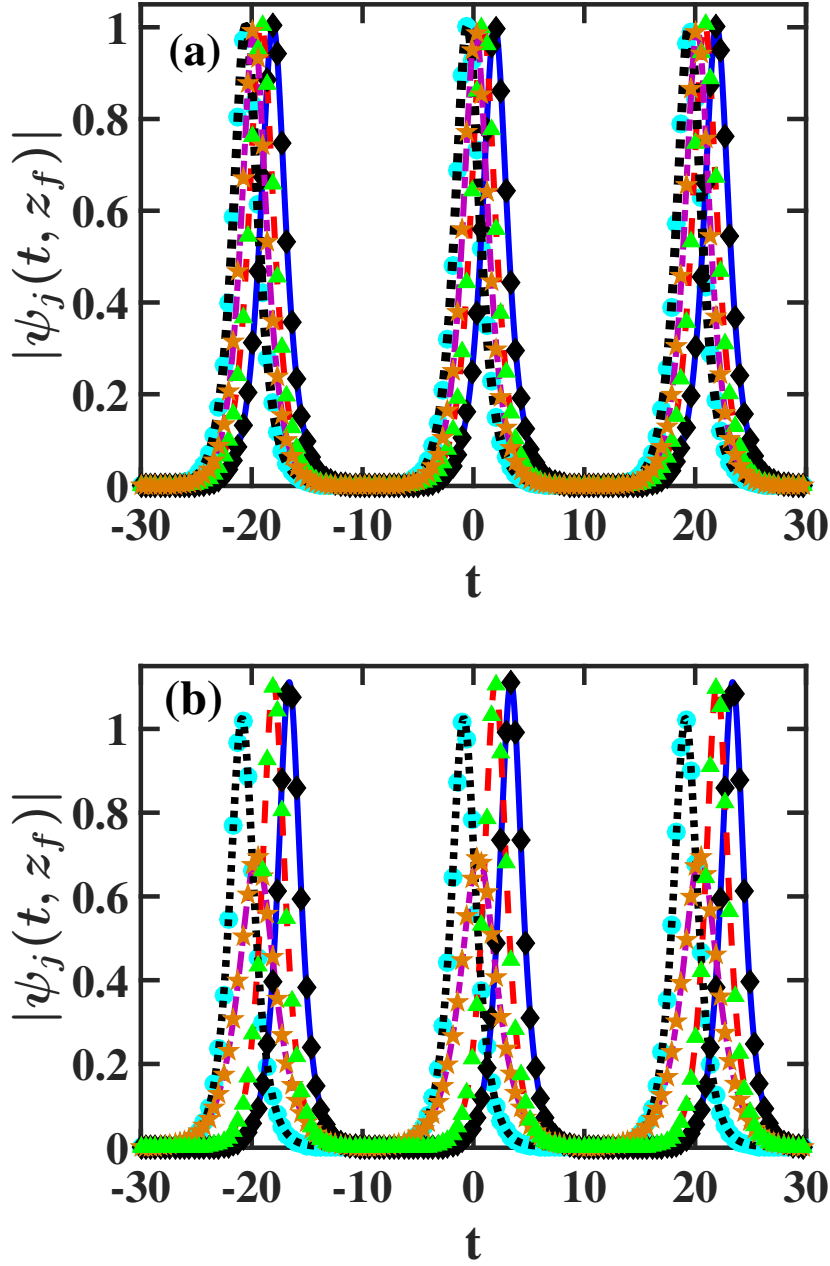


FIG. 8: (Color online) The pulse patterns at the final propagation distance $|\psi_j(t, z_f)|$, where $z_f = 5000$, for the four-sequence transmission system of subsection III D with $\mu = 0.85$ (a) and $\mu = 0.98$ (b). The parameter values are the same as in Fig. 7. The solid blue, dashed red, dash-dotted purple, and dotted black curves correspond to $|\psi_j(t, z_f)|$ with $j = 1, 2, 3, 4$, obtained by numerical simulations with Eq. (1). The black diamonds, green triangles, orange stars, and cyan circles correspond to the theoretical prediction, obtained by summation over fundamental NLS solitons.

- [9] A. Peleg, Q.M. Nguyen, and T.P. Tran, *Opt. Commun.* **380**, 41 (2016).
- [10] Q.M. Nguyen and A. Peleg, *Opt. Commun.* **283**, 3500 (2010).
- [11] A. Peleg, Q.M. Nguyen, and Y. Chung, *Phys. Rev. A* **82**, 053830 (2010).
- [12] A. Peleg and Y. Chung, *Phys. Rev. A* **85**, 063828 (2012).
- [13] D. Chakraborty, A. Peleg, and J.-H. Jung, *Phys. Rev. A* **88**, 023845 (2013).
- [14] Q.M. Nguyen, A. Peleg, and T.P. Tran, *Phys. Rev. A* **91**, 013839 (2015).
- [15] J. Guckenheimer and P.J. Holmes, *Nonlinear Oscillations, Dynamical Systems, and Bifurcations of Vector Fields* (Springer, New York, 1983).
- [16] M. Lakshmanan and S. Rajasekar, *Nonlinear Dynamics* (Springer, Berlin, 2002).
- [17] R.J. Field and M. Burger, eds., *Oscillations and Traveling Waves in Chemical Systems* (Wiley, New York, 1985).
- [18] J.D. Murray, *Mathematical Biology* (Springer, New York, 1989).
- [19] E. Di Cera, P.E. Phillipson, and J. Wyman, *Proc. Natl. Acad. Sci. USA* **86**, 142 (1989).
- [20] M.G. Odell, in *Mathematical models in molecular and cellular biology*, edited by L.A. Segel (Cambridge University Press, Cambridge, England, 1980), Appendix A.3.
- [21] A. Arneodo, P. Couillet, and C. Tresser, *Phys. Lett. A* **79**, 259 (1980).
- [22] A. Arneodo, P. Couillet, J. Peyraud, and C. Tresser, *J. Math. Biology* **14**, 153 (1982).
- [23] K. Tanabe and T. Namba, *Ecology* **86**, 3411 (2005).
- [24] J.A. Vano, J.C. Wildenberg, M.B. Anderson, J.K. Noel, and J.C. Sprott, *Nonlinearity* **19**, 2391 (2006).
- [25] J.P. Preville and K.A. Hoffman, *SIAM Rev.* **55**, 523 (2013).
- [26] A.J. Lotka, *Elements of Physical Biology* (Williams and Wilkins, Baltimore, 1925).
- [27] V. Volterra, *J. Cons. Int. Explor. Mer* **3**, 1 (1928).
- [28] E. Di Cera, P.E. Phillipson, and J. Wyman, *Proc. Natl. Acad. Sci.* **85**, 5923 (1988).
- [29] Y. Li, H. Qian, and Y. Yi, *J. Chem. Phys.* **129**, 154505 (2008).
- [30] Q. Lin, O.J. Painter, and G.P. Agrawal, *Opt. Express* **15**, 16604 (2007).
- [31] The dimensionless distance z in Eq. (1) is $z = X/(2L_D)$, where X is the dimensional distance, $L_D = \tau_0^2/|\tilde{\beta}_2|$ is dispersion length, τ_0 is soliton width, and $\tilde{\beta}_2$ is the second-order dispersion coefficient. The dimensionless time is $t = \tau/\tau_0$, where τ is time. $\psi_j = E_j/\sqrt{P_0}$, where E_j is the electric field of the j th sequence and P_0 is peak power. The dimensionless second-order dispersion coefficient is $d = -1 = \tilde{\beta}_2/(\gamma P_0 \tau_0^2)$, where γ is the Kerr nonlinearity coefficient. The

coefficients ϵ_1 and ϵ_{3jk} are related to the dimensional linear and cubic gain-loss coefficients ρ_1 and ρ_{3jk} by $\epsilon_1 = 2\tau_0^2\rho_1/|\tilde{\beta}_2|$ and $\epsilon_{3jk} = 2\rho_{3jk}/\gamma$. The solitons spectral width is $\nu_0 = 1/(\pi^2\tau_0)$ and the intersequence frequency difference is $\Delta\nu = (\pi\Delta\beta\nu_0)/2$.

- [32] A. Peleg, Q.M. Nguyen, and T.T. Huynh, *Eur. Phys. J. D* **71**, 30 (2017).
- [33] P.C. Becker, N.A. Olsson, and J.R. Simpson, *Erbium-Doped Fiber Amplifiers: Fundamentals and Technology* (Academic, San Diego, CA, 1999), chapter 8.
- [34] Note that the bifurcation parameter μ might appear in the expressions for the $g_j(z)$ or $/$ and in the expressions for the cubic gain-loss coefficients ϵ_{3jk} .
- [35] J. Yang, *Nonlinear Waves in Integrable and Nonintegrable Systems* (SIAM, Philadelphia, 2010).
- [36] J. Coste, J. Peyraud, and P. Couillet, *SIAM J. Appl. Math.* **36**, 516 (1979).